ORIGINAL ARTICLE

Identification of IPF specific genes expressed by lung tissue-derived fibroblasts using next generation sequencing

EUN-JEONG SEO[1*], JONG-UK LEE[1*], SEUNG-LEE PARK[1], MIN-KYUNG KIM[1], JAE-SUNG CHOI[2], HUN-GYU HWANG[3], JUNG-HYUN KIM[4], HUN-SOO CHANG[1], CHOON-SIK PARK[5]

[1]Department of Interdisciplinary Program in Biomedical Science Major, Graduate School, Soonchunhyang University, Asan, Republic of Korea; [2]Division of Respiratory Medicine, Department of Internal Medicine, Soonchunhyang University Cheonan Hospital, Cheonan, Republic of Korea; [3]Soonchunhyang University Bucheon Hospital, Bucheon, Republic of Korea; [4]Division of Allergy and Clinical Immunology, Department of Internal Medicine, Soonchunhyang University Hospital, Seoul, Republic of Korea; [5]Biobank, Soonchunhyang University Bucheon Hospital, Bucheon, Republic of Korea

*These authors contributed equally to this work

ABSTRACT

Background and aim: Idiopathic pulmonary fibrosis (IPF) is a progressive interstitial lung disease characterized by aberrant fibroblast activation and excessive extracellular matrix (ECM) accumulation, resulting in irreversible lung remodeling. Although fibroblasts are central to IPF pathogenesis, comprehensive transcriptomic analyses of IPF patient-derived lung fibroblasts remain limited. This study aimed to identify novel molecular contributors to IPF through transcriptomic profiling of lung fibroblasts.

Methods: We performed total RNA sequencing on primary lung fibroblasts isolated from 33 IPF patients and 10 controls, the latter derived from histologically normal lung tissue adjacent to resected tumors. Differentially expressed genes (DEGs) were identified using trimmed mean of M-values normalization and the Exact test with Bonferroni correction. Gene ontology (GO) enrichment was conducted using DAVID, and network analyses were conducted via STRING and GeneClip3.

Results: GO analysis of 475 DEGs (402 upregulated, 73 downregulated) revealed strong enrichment in ECM-related terms consistently observed across three prior IPF fibroblast datasets. Pathway analysis further implicated cytokine–cytokine receptor interaction, complement and coagulation cascades, and immune-related processes.

Received: 7 August 2025 | Accepted: 5 October 2025

Correspondence: Choon-Sik Park, MD., PhD. / Biobank, Soonchunhyang University Bucheon Hospital, Bucheon, Republic of Korea / Email: mdcspark@daum.net / Hun-Soo Chang, PhD. / Department of Interdisciplinary Program in Biomedical Science Major, Graduate School, Soonchunhyang University, Asan, Republic of Korea / Email: hschang@sch.ac.kr

Network analysis identified *SERPING1, NR4A1*, and *C3* as shared hub genes across both STRING and GeneClip3 platforms. Of the top 20 DEGs, 15 had prior associations with fibrosis, while six (*HSD17B2, HMGCLL1, RASL12, HBG1, LOC105375566 and RIPOR3-AS1*) were novel. *OAS2*, an interferon-stimulated gene, emerged as a novel immune-fibrotic axis component in IPF.

Conclusions: This transcriptomic analysis confirms ECM dysregulation as a core feature of IPF pathogenesis and highlights novel DEGs and hub genes with potential roles in fibrosis, providing a foundation for future functional and translational studies.

Key words: idiopathic pulmonary fibrosis, fibroblasts, gene expression profiling, extracellular matrix

Introduction

Idiopathic pulmonary fibrosis (IPF) is a progressive interstitial lung disease characterized by aberrant activation of fibroblasts and excessive deposition of extracellular matrix (ECM) components such as collagens, elastin, and glycoproteins. These changes disrupt alveolar architecture, increase lung stiffness, and reduce lung volume, a key predictor of mortality (1, 2). In normal wound healing, myofibroblasts are transiently activated and undergo apoptosis after tissue repair. The ECM is largely degraded and replaced with normal tissue, and myofibroblasts are rarely observed in healthy lungs (3, 4). In contrast, IPF is thought to result from aberrant wound healing following repetitive alveolar epithelial injury. Rather than resolving, this process leads to persistent fibroblast activation and progressive fibrosis (1, 5). A key component of this dysfunctional repair is the excessive proliferation of fibroblasts and their differentiation into contractile myofibroblasts, forming fibroblastic foci—a histological hallmark of IPF associated with worse survival (6). Myofibroblast accumulation is driven by both external cues and intrinsic cellular abnormalities. Alveolar epithelial damage triggers the release of profibrotic cytokines, including interleukin-1 (IL-1), tumor necrosis factor-alpha (TNF-α), interleukin-6 (IL-6), and transforming growth factor-beta (TGF-β) (7). In parallel, fibroblasts from IPF lungs exhibit phenotypic alterations, including elevated expression of contractile proteins and enhanced ECM synthesis, relative to fibroblasts from healthy tissue (8). Transcriptomic profiling of IPF-derived fibroblasts offers enables elucidation the molecular mechanisms underlying fibroblast activation and fibrosis progression. To date, three studies have characterized differentially expressed genes (DEGs) in fibroblasts isolated from IPF lung tissue: GSE180415 identified 716 DEGs (419 upregulated and 297 downregulated) (9); GSE17978 reported 1,363 DEGs (10); and a meta-analysis of GSE1724, GSE10921, GSE44723, and GSE40839 identified 227 DEGs (114 upregulated, 113 downregulated) (11) as illustrated in the Venn diagram (Figure S1a). Nevertheless, only two genes — SECTM1 and RPB1 — exhibited consistent differential expression across all three studies (Table S1), reflecting limited reproducibility. Similarly, GO enrichment analysis yielded 19 overlapping terms between pairs of studies, but none were shared across all three (Table S2, Figure S1b). Such discrepancies may stem from small sample sizes and heterogeneous study designs: Hanmandlu et al analyzed nine samples (5 IPF, 4 controls), and Emblom-Callahan et al used 18 (12 IPF, 6 controls). The Plantier et al combined 40 samples from four datasets. Furthermore, demographic and anatomical differences added variability. These limitations highlight the need for transcriptomic studies with larger, clinically consistent cohorts to improve reproducibility and refine our understanding of IPF pathogenesis. Here, we performed next-generation RNA sequencing (RNA-seq) on cultured lung-derived fibroblasts from a relatively large cohort of 33 IPF patients and 10 controls. We then identified DEGs and performed functional enrichment and network analyses to

characterize fibroblast-specific transcriptional changes. Comparative analysis with three previously published IPF fibroblast datasets indicated robust, reproducible ECM-related signatures and uncovered novel candidate genes not previously implicated in IPF, offering new insights into the molecular mechanisms of fibroblast activation and fibrosis progression.

Materials and methods

Study subjects

Lung fibroblasts from patients with IPF were obtained from the biobank of Soonchunhyang University Hospital (Bucheon, Korea), following Institutional Review Board approval (IRB numbers: SCHCA-IRB-2018-10-034 and 201910-BR-058). Informed written consent was obtained from all participants. Subjects underwent clinical evaluation, including medical history review, chest X-ray, high-resolution computed tomography, and pulmonary function testing. Patients with evidence of collagen vascular diseases were excluded. The diagnosis of IPF was established according to the 2011 and 2018 ATS/ERS/JRS/ALAT guidelines (12).

Fibroblast culture

Primary lung fibroblasts were isolated from surgical biopsy specimens from 33 patients with histologically confirmed usual interstitial pneumonia, and from histologically normal lung tissue of 10 patients who underwent resection for stage I or II lung cancer. Fibroblast culture protocols followed previously published methods (13). Briefly, tissues were minced and cultured in 150 cm^2 flasks containing Dulbecco's Modified Eagle Medium (Lonza), 10% fetal bovine serum (Thermo Fisher Scientific), 2 mmol/L glutamine, and 1% penicillin-streptomycin-amphotericin B (Lonza). Cultures were maintained at 37°C in a 5% CO□ incubator and serially passaged to obtain a morphologically homogeneous population of adherent fibroblasts.

Total RNA sequencing

Total RNA extraction and sequencing were performed by Macrogen Inc. (Seoul, Korea), following previously described protocols (14). Total RNA was extracted from lung fibroblasts using TRIzol reagent (Invitrogen). RNA concentration was measured using Quant-iT RiboGreen RNA Assay Kit (Invitrogen, #R11490), and RNA integrity was assessed with the Agilent TapeStation RNA ScreenTape (Agilent, #5067-5576). Only RNA samples with an RNA integrity number > 7.0 were used for library preparation. For each sample, 0.5 μg of total RNA was used to prepare a library using the Illumina TruSeq Stranded Total RNA Library Prep Gold Kit (#20020599). Ribosomal RNA was depleted, and the remaining RNA was fragmented by divalent cations under elevated temperature. First-strand cDNA synthesis was performed using SuperScript II reverse transcriptase (Invitrogen, #18064014) and random primers, followed by second-strand synthesis using DNA polymerase I, RNase H, and dUTP. The resulting cDNA fragments underwent end repair, A-tailing, and adapter ligation. Libraries were purified and PCR-amplified to yield the final cDNA libraries. Library quality and concentration were assessed using the KAPA Library Quantification Kit (KAPA BIOSYSTEMS, #KK4854) and Agilent TapeStation D1000 ScreenTape (#5067-5582). Libraries were sequenced on the Illumina NovaSeq platform (paired-end, 2 × 100 bp).

RNA-seq data processing

Raw sequencing data quality was assessed with FastQC (https://www.bioinformatics.babraham.ac.uk/projects/fastqc/). Adapter sequences and low-quality reads (Phred score < Q20) were trimmed using FASTX_Trimmer (http://hannonlab.cshl.edu/fastx_toolkit/) and BBMap (https://sourceforge.net/projects/bbmap/). Clean reads were aligned to the human reference genome using TopHat (15). Gene expression was quantified using BEDTools (16), and Cufflinks (17), and normalized using EdgeR in R (https://www.r-project.org). Trimmed mean of M-values (TMM) was applied, and expression was presented as log2 counts per million. Trimmed mean of M-values (TMM) was applied, and expression was presented as log2 counts per million. DEGs were identified using the Exact test in EdgeR, and statistical significance was determined using Bonferroni-adjusted p-values (< 0.05).

The RNA-seq data have been deposited in NCBI Gene Expression Omnibus under accession number GSE301181.

Gene ontology and pathway enrichment analysis

Functional enrichment of DEGs was performed using DAVID (Database for Annotation, Visualization, and Integrated Discovery) v6.8 tool (18). GO terms were classified into Biological Process (BP), Cellular Component (CC), and Molecular Function (MF) based on the GO database (19). Enrichment was also assessed using KEGG and REACTOME pathways integrated in DAVID. Statistical significance for enrichment was evaluated using the false discovery rate (FDR) correction, with FDR-adjusted p-values < 0.05 considered significant.

Network analysis

Interaction networks were generated using GeneClip3 (http://cismu.net/genclip3/analysis.php) and STRING v2.2.0 (confidence cutoff = 0.4) via Cytoscape v3.10.3. Network clustering and module detection were performed using MCODE v2.0.3 in Cytoscape.

Statistical analysis

Statistical analyses were conducted using SPSS (IBM). Data normality was assessed using the Shapiro–Wilk test. Continuous variables were expressed as mean ± standard deviation or median with interquartile range. Group comparisons were performed using independent t-tests or Mann–Whitney U tests as appropriate. Categorical variables were compared using Pearson's Chi-square test. A two-tailed p-value < 0.05 was considered statistically significant.

Results

Patient characteristics

Clinical characteristics of the study participants are summarized in Table 1. A total of 43 individuals were included in the analysis, comprising 33 patients with IPF and 10 controls. The mean age was higher in the IPF group than in the control group, although this difference did not reach statistical significance (p=0.081). Sex distribution and smoking status were comparable between the two groups. In contrast, pulmonary function parameters showed significant impairment in the IPF group. The median predicted forced vital capacity was significantly lower in IPF patients compared to controls (p=0.010). Similarly, the median predicted diffusion capacity for carbon monoxide was markedly reduced in the IPF group relative to controls (p=0.002).

Table 1. Clinical characteristics of the study subjects.

Variable	Control	IPF	p-value
No.	10	33	-
Age (year)	58.4±9.2	64.3±9.2	0.081
Sex (male/female)	4/6	15/18	0.761
Smoke (NS/ES/SM)	7/1/2	16/6/11	0.489
FVC (% pred.)	89.5 (81.8–105.5)	69(58–83)	0.01
DL_{CO} (% pred.)	85(76–92.5)	47.5(0–69)	0.002
Death/ Survival	2/8	13/20	0.26

Values are presented as median (interquartile range) or mean ± standard error of the mean. *Abbreviations:* IPF: idiopathic pulmonary fibrosis; NS/ES/SM: non-smokers, ex-smokers, smokers; FVC: forced vital capacity; DL_{CO}: diffusion capacity of the lung for carbon monoxide.

Differentially expressed genes in IPF fibroblasts compared to controls

From the initial dataset comprising 46,427 genes, we excluded 31,375 genes with fewer than 10 read counts and applied TMM normalization to the remaining 15,252 genes. Based on the criteria of $|FC| \geq 2$ and adjusted p (Bonferroni) < 0.05, a total of 475 genes were identified as differentially expressed, including 402 upregulated and 73 downregulated in IPF fibroblasts. (Figure S2). Volcano plot and hierarchical clustering heat map of these genes are presented in Figure 1. The complete gene list is provided in Table S3.

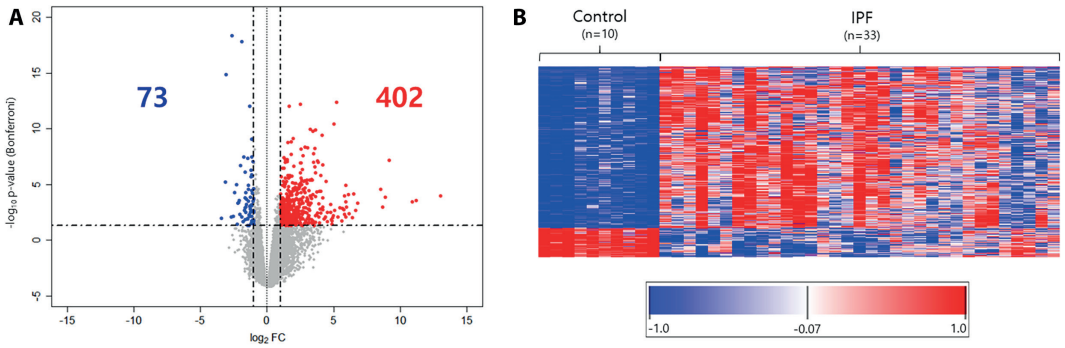

Figure 1. Differential gene expression analysis of lung tissues - derived fibroblasts between 33 IPF patients and 10 controls. (a) Volcano plot displaying differential expression of 15,252 genes in lung fibroblasts, highlighting 402 significantly upregulated (red) and 73 downregulated (blue) genes in IPF compared to controls (cutoff: |fold change| > 2, Bonferroni adjusted *p*-value < 0.05). (b) Hierarchical clustering heatmap of 475 differentially expressed genes, demonstrating distinct expression profiles. *Abbreviations:* IPF: idiopathic pulmonary fibrosis; log2FC: log fold change of IPF/control.

The top 20 genes with the highest FC values are listed in Table 2. Among them, eight genes—*BMP5, TMEM176B, C7, GDF10, ADAMTS8, EDNRB, FGFR4*, and *TNFSF15*—are associated with the development of IPF (20-27). Five genes-including *ADH1B, ADH1A, EDNRB, GDF10,* and *FGFR4* have been linked to liver fibrosis (28-32), while *SCUBE1* and *NKD2* are associated with kidney fibrosis (33, 34). *ADAMTS8* and *ADAMTS19* are implicated in cardiac and skin fibrosis, respectively (35, 36) and *CFTR* and *TNFSF15* are connected to cystic and colonic fibrosis (37, 38). In contrast, *HSD17B2*, *HMGCLL1*, *RASL12*, *HBG1*, the noncoding RNA *RIPOR3-AS1*, and the predicted gene *LOC105375566* have not yet been studied in the context of fibrosis.

Gene ontology analysis

In gene ontology analysis of the 475 DEGs, 463 were recognized by the DAVID v6.8 database (https://david.ncifcrf.gov/) and included in the functional enrichment analysis. FDR-adjusted p-values < 0.05 considered significant. A total of 21 GO terms were identified across the three major GO categories: 8 in BP, 8 in CC, 1 in MF and 4 in KEGG pathway. Out of 402 up-regulated DEGs, 392 were used for GO analysis. A total of 21 GO terms were identified across the three major GO categories: 7 in BP, 8 in CC, 2 in MF, 4 in KEGG, and 4 in REACTOME pathway. Out of 73 down-regulated DEGs, 71 were used for GO analysis. None of GO terms were identified. The full list of GO annotations, along with associated gene sets, is provided in Table S4. Both 475 total DEGs and 402 up-regulated DEGs presented the top five significantly enriched GO terms as extracellular region (GO:0005576), extracellular space (GO:0005615), plasma membrane (GO:0005886), collagen-containing extracellular matrix (GO:0062023), and extracellular exosome (GO:0070062) (Table 3). These GO terms primarily reflect processes and components related to ECM organization and localization, which are known to play critical roles in the pathogenesis of IPF. Moreover, there were 4 shared KEGG pathways between 475 DEGs and 402 DEGs: complement and coagulation cascades (hsa04610), cytokine-cytokine receptor interaction (hsa04060), rheumatoid arthritis (hsa05323), and staphylococcus aureus infection (hsa05150). 402 up-regulated DEGs also exhibited 4 REACTOME pathways: Immune system (R-HSA-168256), extracellular matrix organization (R-HSA-1474244), molecules associated with elastic fibers (R-HSA-2129379) and elastic fiber formation (R-HSA-1566948) as shown in Table S4.

Comparative analysis of DEGs and GOs with previous studies

We compared the 475 DEGs identified in our study with those reported in three previously published gene expression data of IPF fibroblasts (GSE180415

Table 2. Top 20 differentially expressed genes with the highest absolute fold change between 33 IPF and 10 control fibroblasts.

Gene	Control	IPF	log_2FC	*p*-value (Bonferroni)	Implication in fibrosis	Reference
BMP5	0.02±0.04	2.7±2.58	11.18	2.700.E-04	IPF	20
TMEM176B	0±0	1.07±1.44	10.91	3.721.E-04	IPF	21
C7	0±0.01	1.18±1.18	9.15	6.985.E-08	IPF	22
GDF10	0.09±0.12	1.7±1.62	6.41	9.334.E-03	IPF, liver	23, 31
EDNRB	0.53±0.94	4.43±2.03	5.92	3.477.E-04	IPF, liver	25, 30
FGFR4	0.24±0.21	2.6±1.77	5.91	1.144.E-05	IPF, liver	26, 32
ADAMTS8	0.91±0.7	4.35±2.67	6.08	7.672.E-05	IPF, heart	24, 35
TNFSF15	0.37±0.3	2.64±1.71	5.81	9.899.E-05	IPF, colon	27, 38
ADH1B	0.46±0.67	3.84±2.48	6.63	2.044.E-03	liver	28
ADH1A	0.04±0.07	0.97±1.13	5.93	7.946.E-03	liver	29
SCUBE1	0±0	1.42±1.81	13.03	1.005.E-04	kidney	33
NKD2	0.01±0.02	1.21±1.27	8.54	2.562.E-05	kidney	34
CFTR	0±0.01	0.81±1.08	8.68	1.124.E-03	cystic fibrosis	37
ADAMTS19	0.13±0.18	2.02±1.59	5.96	1.092.E-03	skin	36
HSD17B2	0.02±0.06	1.83±1.83	8.88	1.335.E-04	N/A	N/A
HMGCLL1	0.04±0.07	1.49±1.37	6.79	4.835.E-04	N/A	N/A
HBG1	0.02±0.03	0.65±0.78	6.13	4.057.E-03	N/A	N/A
RASL12	0.14±0.2	2.36±1.78	6.47	6.650.E-05	N/A	N/A
RIPOR3-AS1	0.05±0.06	0.97±1.02	5.77	1.800.E-03	N/A	N/A
LOC105375566	0.04±0.06	1.03±0.96	5.81	4.515.E-03	N/A	N/A

Values are presented as mean ± standard error of the mean. *p*-values shown are Bonferroni-adjusted values from the Exact test. *Abbreviations:* IPF: idiopathic pulmonary fibrosis; log_2FC: fold change of IPF/Control; FDR: false discovery rate; DOI: digital object identifier; N/A: not applicable.

Table 3. Top five significantly enriched GO terms among DEGs from our IPF fibroblast dataset and overlap DEGs of four studies.

Gene	Term ID	Category	Term name	Count	Fold Enrichment	FDR
Total DEGs of our study (475 genes)	GO:0005576	CC	extracellular region	98	2.21	1.413E-11
	GO:0005615	CC	extracellular space	77	2.15	3.258E-08
	GO:0005886	CC	plasma membrane	159	1.48	1.708E-06
	GO:0062023	CC	collagen-containing extracellular matrix	24	3.23	1.516E-04
	GO:0070062	CC	extracellular exosome	74	1.72	2.560E-04
Up-regulated genes of our study (402 genes)	GO:0005576	CC	extracellular region	92	2.45	8.954E-14
	GO:0005615	CC	extracellular space	73	2.41	3.337E-10
	GO:0005886	CC	plasma membrane	132	1.46	8.095E-05
	GO:0062023	CC	collagen-containing extracellular matrix	22	3.51	1.118E-04
	GO:0070062	CC	extracellular exosome	66	1.82	1.230E-04

Gene	Term ID	Category	Term name	Count	Fold Enrichment	FDR
Overlap DEGs of four studies # (85genes)	GO:0005576	CC	extracellular region	29	3.30	5.696E-07
	GO:0005615	CC	extracellular space	26	3.67	5.696E-07
	GO:0062023	CC	collagen-containing extracellular matrix	8	5.44	2.633E-02
	GO:0009897	CC	external side of plasma membrane	8	5.10	2.891E-02
	GO:0031012	CC	extracellular matrix	6	7.08	3.852E-02

#: GSE180415 (Hanmandlu et al. 2022) and GSE17978 (Emblom-Callahan et al. 2010) and GSE1724, 10921, 44723, 40839 (Plantier et al. 2016) and our study. Enrichment significance values correspond to FDR-adjusted *p*-values (FDR < 0.05). *Abbreviations:* GO: gene ontology; DEG: differentially expressed gene; IPF: idiopathic pulmonary fibrosis; GSE: gene expression omnibus series; FDR: false discovery rate; CC: cellular component.

Table 4. A list of 85 differentially expressed genes shared across four studies.

Study	No of overlap genes	Gene
GSE180415 & our data	38	*CEMIP, PAPPA, TFPI2, RSPO3, VAMP8, DPP4, SERPING1, ICAM1, MAN1C1, SELENOP, SCARA3, EXPH5, CYP1B1, GPNMB, F11R, ADGRD1, EFEMP1, ADAMTS14, GASK1B, PURPL, SLC2A9, IGSF10, ADAMTS19, SEZ6L2, PLEKHH2, NES, LINC02015, OXTR, PTGS1, DPP4-DT, MEDAG, FAM43A, BMP2, CFD, LINC01936, GRIK4, IL13RA2, LRRN4CL*
GSE1724, 10921, 44723, and 40839 & our study	29	*FSTL3, UBL3, AMIGO2, PRSS3, KIAA1217, TRANK1, IL1R1, SESN1, TNFAIP2, VWA5A, IFITM3, TMEM140, IFITM1, TNFRSF1B, BTN3A2, HLA-DMB, OAS2, ASPA, MME, CBR3, BTN3A3, CXCL2, DOCK4, PSMB9, PTGES, TNFRSF14, DHX58, ARHGAP28, NR1H3*
GSE17978 & our study	13	*SSH2, AMPD3, ADM, CDKN2D, FBXO32, GDF15, FBLN1, GPRC5B, TGFB3, C1S, CTSK, ANTXR1, MOXD1*
GSE180415 & GSE17978 & our data	4	*LAMA4, RARRES2, PTGDS, CPZ*
GSE180415 & GSE1724, 10921, 44723, and 40839 & our data	1	*TNFRSF21*

A table shows the genes shared with between our study and three other studies: GSE180415 (Hanmandlu et al. 2022) and GSE17978 (Emblom-Callahan et al. 2010) and GSE1724, 10921, 44723, 40839 (Plantier et al. 2016). *Abbreviation:* GSE: gene expression omnibus series.

(9), GSE17978 (10) and GSE1724, 10921, 44723, and 40839 (11). A total of 85 DEGs were identified as overlap genes among four studies (Table 4). Table S5 showed the GO analysis result of 85 DEGs. There were the five GO terms and one KEGG pathway such as extracellular region (GO:0005576), extracellular space (GO:0005615), collagen-containing extracellular matrix (GO:0062023), external side of plasma membrane (GO:0009897), extracellular matrix (GO:0031012), extracellular matrix organization (R-HSA-1474244), and cytokine-cytokine receptor interaction (hsa04060). Notably, the result shared the top three GO terms of our study such as extracellular region (GO:0005576), extracellular space

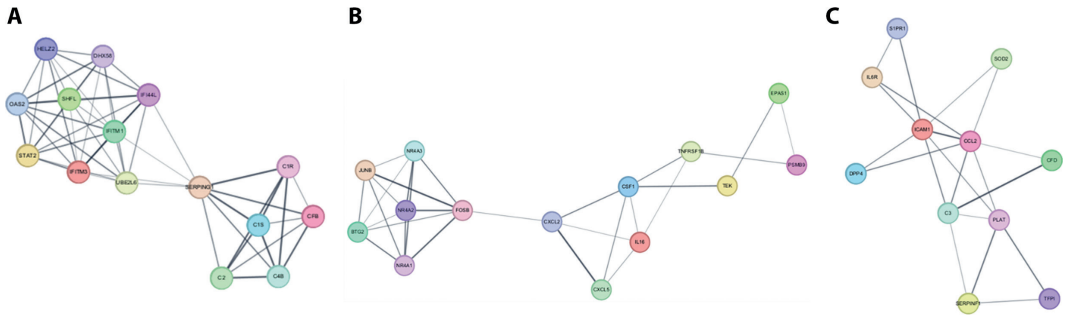

Figure 2. Protein-protein interaction network analysis and cluster of 475 differentially expressed genes by STRING and MCODE. (a-c) Cluster 1=15 nodes, 54 edges, score:7.7, cluster 2=14 nodes, 28 edges, score:4.3, cluster 3=11 nodes, 20 edges, score:4.

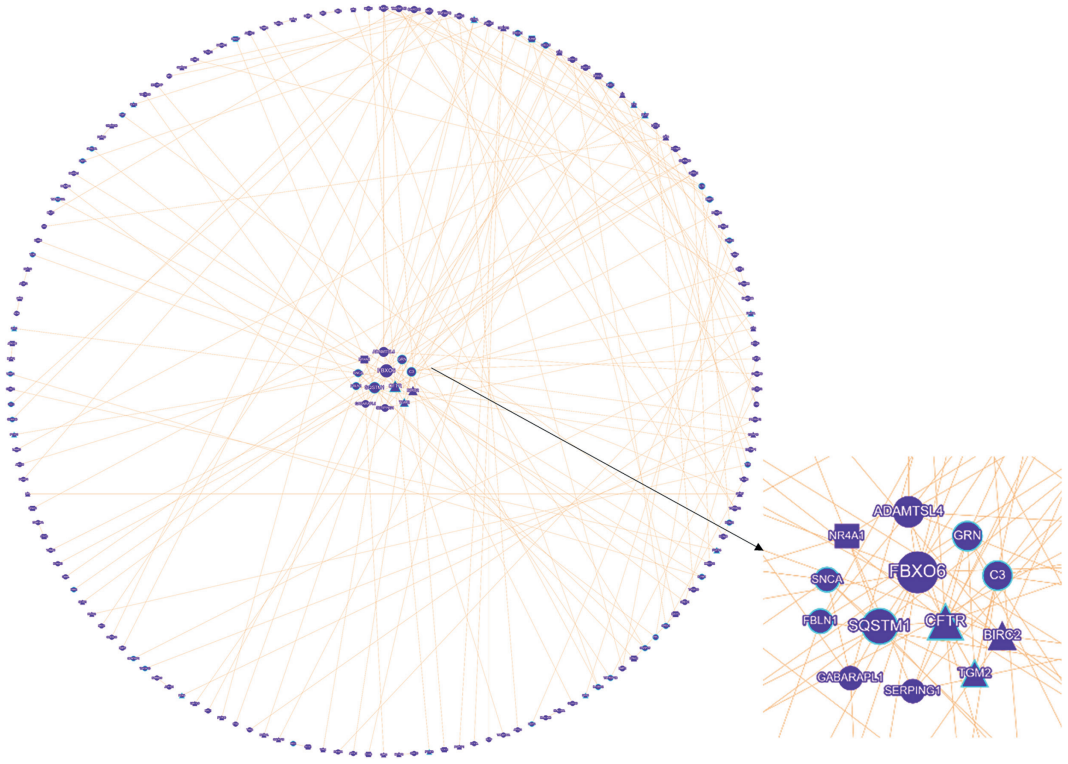

Figure 3. Functional gene association network of 475 differentially expressed genes via GeneClip3. Circle: gene; square: transcription factor; triangle: enzyme; sky blue mark on shapes: already known as IPF related genes.

(GO:0005615), and collagen-containing extracellular matrix (GO:0062023) as top GO terms with other two ECM related GO terms (Table 3).

Network analysis

STIRNG analysis of 475 DEGs identified 410 nodes and 726 edges, where MCODE made 3 clusters (score≥4, Figure 2). 437 DEGs within 475 were employed for the GeneClip3 analysis based on the number of functional connections (degree) within the literature- and GO-based interaction network (39). The top ~3% of nodes by degree were defined as hubs (Figure 3). Three genes, *SERPING1*, *NR4A1* and *C3*, were concurrently shown in two analyses. Gene and protein network (8 node, 14 edges, score=4) of 85 shared DEGs

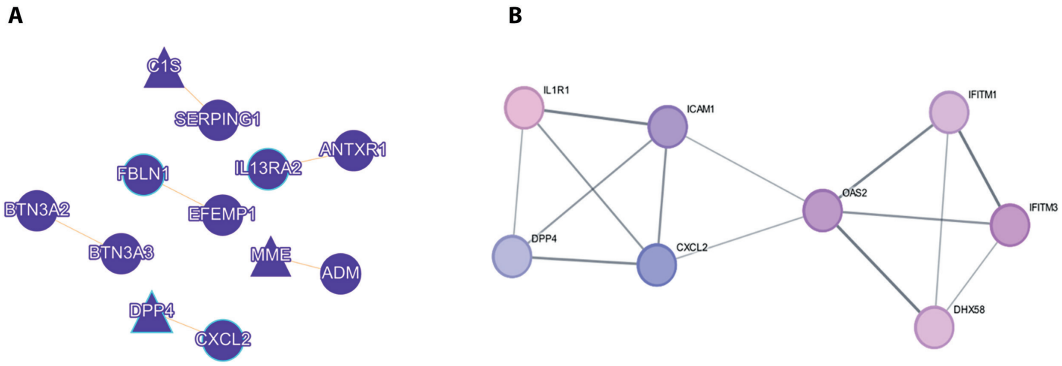

Figure 4. Network analysis of 85 differentially expressed genes. (a) gene network and (b) protein network analysis of overlapping genes among 4 studies. Circle: gene; square: transcription factor; triangle: enzyme; sky blue mark on shapes: already known as IPF related genes.

in 4 studies indicated that two well-known IPF related genes, *DPP4* and *CXCL2* (Figure 4).

Discussion

Our large□scale RNA□seq analysis of IPF lung fibroblasts identified 475 DEGs, with a strong enrichment of GO terms related to ECM organization and localization. Among the top five GO terms were extracellular region (GO:0005576), extracellular space (GO:0005615), and collagen-containing extracellular matrix (GO:0062023). Comparative analysis with three previous IPF fibroblast transcriptomic datasets revealed that, although only 85 DEGs and 14 GO terms overlapped with any of the prior studies and no single gene was common to all (Figure S3), these ECM-related GO terms consistently emerged across datasets (Tables S4-6). This convergence, despite differences in sample origin, cohort size, and analytical pipelines, underscores the robustness and disease relevance of ECM remodeling as a central process in IPF fibroblasts. Among the enriched pathways, the cytokine–cytokine receptor interaction (hsa04060) pathway was consistently activated across all four datasets. This underscores the central role of cytokine signaling in fibroblast activation and intercellular communication in the fibrotic lung microenvironment. Profibrotic cytokines such as IL-1β, IL-6, TNF-α, and TGF-β1 sustain myofibroblast activation and ECM deposition (40). The recurrent enrichment of this pathway suggests that fibroblasts may both respond to and contribute to the local cytokine milieu, promoting persistent fibrotic remodeling. In addition to cytokine signaling, three immune- and inflammation-associated pathways—complement and coagulation cascades (hsa04610), rheumatoid arthritis (hsa05323), and Staphylococcus aureus infection (hsa05150)—were also enriched. The complement pathway has been implicated in IPF progression, with elevated levels of C3, C5, and C5–C9 complexes correlating with disease severity in plasma and bronchoalveolar lavage fluid (41). The rheumatoid arthritis (RA) pathway enrichment highlights shared molecular mechanisms between IPF and RA-associated interstitial lung disease, both of which often present with usual interstitial pneumonia patterns (42). Triggianese et al proposed that complement activation, fibroblast activation, and pro-inflammatory cytokine signaling are common mechanisms in both diseases (43). Enrichment of the Staphylococcus aureus infection pathway is notable, as colonization has been associated with acute exacerbations and poor prognosis in IPF (44). Altered ECM structure and immune dysfunction may facilitate bacterial persistence, and fibroblast responses to microbial components may further exacerbate fibrosis. Network analysis identified *SERPING1*, *NR4A1*, and *C3* as hub genes in STRING and GeneClip3-based networks, indicating their central roles in fibroblast regulatory circuits. *SERPING1* has been reported as a serum biomarker in IPF (45); *NR4A1* modulates TGF-β signaling and suppresses fibrosis in several organs (46); and

C3-deficient mice are partially protected from bleomycin-induced fibrosis (47). These genes were upregulated in primary IPF fibroblasts, supporting their relevance to IPF pathology. Analysis of the 85 shared DEGs revealed a subnetwork including *CXCL2*, linked to *IL1R1*, *ICAM1*, and *OAS2*. While *IL1R1* and *ICAM1* are established pro-fibrotic mediators (48, 49), *OAS2*, an interferon (IFN)-induced gene with antiviral function (50), has not been studied in IPF. Emerging evidence has implicated interferon signaling in IPF pathogenesis, with single-cell RNA-seq studies showing elevated IFN-γ activity in immune cells in fibrotic lungs (51, 52). Importantly, these studies revealed that interferon-activated immune cells are often positioned near fibroblast-rich regions. This physical closeness makes it easier for immune-derived cytokines and paracrine signals to directly influence fibroblast behavior, including activation and extracellular matrix production. Such immune–fibrotic interplay suggests that OAS2-driven interferon responses could shape fibrogenic remodeling in IPF, highlighting a potential translational link between antiviral defense programs and fibrosis (53). Notably. of the 457 DEGs identified in our study, 399 were not found in any of the three datasets. Several of these genes — *BMP5, TMEM176B, C7, GDF10, ADAMTS8, EDNRB, FGFR4*, and *TNFSF15* — are known to participate in fibrosis in other organs such as the liver, kidney, and heart, suggesting conserved fibrogenic pathways across tissues. We also uncovered several novel genes not previously linked to IPF, including *ADH1A, ADH1B, SCUBE1, NKD2, CFTR, ADAMTS19, HSD17B2, RASL12*, *HMGCLL1, HBG1* and the long non-coding RNA *RIPOR3-AS* and *LOC105375566*. These genes may represent new regulators of fibroblast activation or matrix remodeling. *ADH1A, ADH1B, SCUBE1*, *NKD2*, *CFTR*, and *ADAMTS19* are associated with liver, renal, cystic fibrosis, and skin fibrosis (28, 29, 33, 34, 36, 37) but haven't been studied in IPF. *HSD17B2* exhibiting a well-established function in hormone metabolism (54), has recently been reported to be correlated with TGF-β/Snail mediated epithelial-mesenchymal transition in endometriosis (55). This suggests that in fibroblasts *HSD17B2* may contribute EMT-like or mesenchymal gene activation under profibrotic signaling through hormonal regulation. The reported significance of *HMGLL1* in lipid biosynthesis and energy metabolism (56) suggests a plausible link to IPF pathogenesis. By supplying cytosolic acetyl-CoA, *HMGCLL1* may promote histone acetylation and profibrotic gene expression, while simultaneously fueling lipid biosynthesis that predisposes fibroblasts to ferroptotic lipid peroxidation such as 4-hydroxy-2-nonenal, malondialdehyde accumulation). As Xin Geng et al. reported that increasing hemoglobin-oxygen affinity alleviates lung fibrosis in a bleomycin-induced model (57), *HBG1* may be functionally linked to IPF pathology. *RASL12*, a member of Ras-related GTPase, participates in intracellular signaling involved in fibrosis (58). Given that *RIPOR3-AS1* was recently discovered as senescence-induced lncRNA (59) and that fibroblast senescence together with metabolic reprogramming are hallmarks of IPF (60, 61), its dysregulation may contribute to disease progression. According to the NCBI Gene database (Gene ID: 105375566), LOC105375566, currently annotated as an uncharacterized lncRNA, is located on chromosome 7q36 in close proximity to TMEM176B (NCBI Gene, Gene ID: 28959, accessed September 17 2025). Since TMEM176B has recently been reported to alleviate pulmonary fibrosis by inhibiting TGF-β/SMAD signaling (21), it is tempting to speculate that LOC105375566 might exert cis-regulatory effects on nearby genes. However, genomic proximity alone does not imply functional relatedness, and direct experimental evidence is still lacking. In addition, we observed dysregulation of genes involved in organ development (*GLDN*), wound healing (*DMKN*), and ion transport (*KCNJ2*, *KCND1/2/3*, *KCNE3, KCNG*) that have not been characterized in IPF. Similar changes in developmental regulators and potassium channels were noted in previous methylation and transcriptome studies (9), suggesting that fibroblasts may acquire aberrant features beyond matrix production, potentially due to epigenetic reprogramming. Several limitations must be considered. First, the use of stringent criteria (Bonferroni-adjusted $p<0.05$ and $|FC|>2$), may have excluded genes with modest but biologically relevant expression changes. Future studies employing more permissive thresholds or machine learning–based feature selection could uncover additional candidates. Second, although primary fibroblast cultures enable

cell type–specific transcriptomic profiling, in vitro expansion may lead to phenotypic drift or overrepresentation of specific subpopulations, limiting fidelity to the in vivo microenvironment. Third, control fibroblasts were derived from histologically normal lung tissue adjacent to resected tumors. This pragmatic approach is widely adopted in human studies, but the possibility of subtle transcriptional alterations related to the tumor microenvironment cannot be completely excluded. Finally, our gene ontology analysis using the DAVID database depends on existing annotations and may overlook under-characterized pathways. Nevertheless, the consistent enrichment of ECM-related terms across our and previous datasets reinforces the biological validity of our findings. Future studies should prioritize functional validation of novel DEGs identified in our analysis. Gene silencing or overexpression experiments in fibroblasts could determine their roles in collagen deposition, myofibroblast differentiation, and cell migration. Single-cell RNA-seq may reveal whether these genes are enriched in specific fibroblast subsets. Integration with epigenomic and proteomic data may reveal upstream regulatory mechanisms and therapeutic targets. Clinically, correlation of gene expression with patient survival or treatment response could inform biomarker discovery. In summary, this transcriptomic analysis of primary lung fibroblasts provides a cell-type–specific view of IPF-associated transcriptional remodeling. Our findings confirm the central role of ECM dysregulation and identify numerous novel candidate genes that expand our understanding of fibroblast heterogeneity and activation in IPF. These data offer a valuable resource for future mechanistic and translational research aimed at improving IPF diagnosis and treatment.

Acknowledgements: This research was supported by Basic Science Research Program through the National Research Foundation of Korea (NRF) funded by the Ministry of Education (RS202300240858). The biospecimens and data used for this study were provided by the Biobank of Soonchunhyang University Bucheon Hospital, a member of the Korea Biobank Network (KBN4_A06). We would like to thank Myung-Ran Lee, Young-Gil Lee, Jeong-Eun Lee, and Da-Jeong Jang for their assistance in the collection and distribution of biospecimens and their clinical information.

Funding: This research was supported by Basic Science Research Program through the National Research Foundation of Korea (NRF) funded by the Ministry of Education (RS202300240858, RS202400462943). The biospecimens and data used for this study were provided by the Biobank of Soonchunhyang University Bucheon Hospital (KBN4_A06), a member of the Korea Biobank Network.

Conflict of Interests: Each author declares that he or she has no commercial associations (e.g., consultancies, stock ownership, equity interest, patent/licensing arrangement etc.) that might pose a conflict of interest in connection with the submitted article.

Data Availability: The RNA-seq datasets generated and/or analyzed during the current study have been deposited in the NCBI Gene Expression Omnibus (GEO) under accession number GSE301181.

Ethics Approval: This study was performed in line with the approval from the Institutional Review Board (IRB numbers: SCHCA-IRB-2018-10-034 and 201910-BR-058).

Consent to Participate: Informed consent was obtained from all individual participants included in the study.

Consent to Publish: Informed written consent was obtained from all participants.

Declaration on the Use of AI: None

Authors' Contributions: EJS, JUL, CSP, HSC: Conceptualization; EJS, JUL, MKK: Data curation; JUL, CSP: Funding acquisition; JUL, CSP, HSC, JSC: Methodology; EJS, JUL: Validation; EJS, JUL, SLP: Visualization; EJS, JUL, HGH, JHK, CSP, HSC: Writing – original draft; all authors: Writing – review & editing.

References

1. Lederer D, Martinez F. Idiopathic pulmonary fibrosis. N Engl J Med. 2018;378(19):1811–23.
2. Demirkol B, Gul S, Cortuk M, Akanil Fener N, Yavuzsan E, Eren R, et al. Protective efficacy of pirfenidone in rats with pulmonary fibrosis induced by bleomycin. Sarcoidosis Vasc Diffuse Lung Dis. 2023;40(3):e2023036.

3. Upagupta C, Shimbori C, Alsilmi R, Kolb M. Matrix abnormalities in pulmonary fibrosis. Eur Respir Rev. 2018;27(148):180033.
4. Chilosi M, Doglioni C, Murer B, Poletti V. Epithelial stem cell exhaustion in the pathogenesis of idiopathic pulmonary fibrosis. Sarcoidosis Vasc Diffuse Lung Dis. 2010;27(1):7-18.
5. Cilli A, Uzer F. Disease progression in idiopathic pulmonary fibrosis under anti-fibrotic treatment. Sarcoidosis Vasc Diffuse Lung Dis. 2023;40(3):e2023034.
6. Nicholson A, Fulford L, Colby T, du Bois R, Hansell D, Wells A. The relationship between individual histologic features and disease progression in idiopathic pulmonary fibrosis. Am J Respir Crit Care Med. 2002;166(2):173–7.
7. Selman M, Pardo A. Alveolar epithelial cell disintegrity and subsequent activation: a key process in pulmonary fibrosis. Am J Respir Crit Care Med. 2012;186(2):119–21.
8. Crestani B, Marchand-Adam S, Fabre A, Dehoux M, Soler P. Fibroblasts: the missing link between fibrotic lung diseases of different etiologies? Respir Res. 2013;14(1):81.
9. Hanmandlu A, Zhu L, Mertens T, Collum S, Bi W, Xiong F, et al. Transcriptomic and epigenetic profiling of fibroblasts in idiopathic pulmonary fibrosis. Am J Respir Cell Mol Biol. 2022;66(1):53–63.
10. Emblom-Callahan M, Chhina M, Shlobin O, Ahmad S, Reese E, Iyer E, et al. Genomic phenotype of non-cultured pulmonary fibroblasts in idiopathic pulmonary fibrosis. Genomics. 2010;96(3):134–45.
11. Plantier L, Renaud H, Respaud R, Marchand-Adam S, Crestani B. Transcriptome of cultured lung fibroblasts in idiopathic pulmonary fibrosis: Meta-analysis of publically available microarray datasets reveals repression of inflammation and immunity pathways. Int J Mol Sci. 2016;17(12):2091.
12. Raghu G, Remy-Jardin M, Myers J, et al. Diagnosis of idiopathic pulmonary fibrosis: an official ATS/ERS/JRS /ALAT clinical practice guideline. Am J Respir Crit Care Med. 2018;198(5):e44–e68.
13. Lee JU, Cheong HS, Shim EY, Bae DJ, Chang HS, Uh ST, et al. Gene profile of fibroblasts identify relation of CCL8 with idiopathic pulmonary fibrosis. Respir Res. 2017;18(1):3.
14. Seo Y, Lee J, Kim K, et al. Gene expression profiling of mouse cavernous endothelial cells for diagnostic targets in diabetes-induced erectile dysfunction. Investig Clin Urol. 2021;62(1):90–9.
15. Trapnell C, Pachter L, Salzberg S. TopHat: discovering splice junctions with RNA-Seq. Bioinformatics. 2009;25(9):1105–11.
16. Quinlan A, Hall I. BEDTools: a flexible suite of utilities for comparing genomic features. Bioinformatics. 2010;26(6):841–2.
17. Roberts A, Trapnell C, Donaghey J, Rinn J, Pachter L. Improving RNA-Seq expression estimates by correcting for fragment bias. Genome Biol. 2011;12(3):R22.
18. Sherman B, Hao M, Qiu J, Jiao X, Baseler M, Lane H, et al. DAVID: a web server for functional enrichment analysis and functional annotation of gene lists (2021 update). Nucleic Acids Res. 2022;50(W1):W216–W21.
19. Consortium TGO, Aleksander S, Balhoff J, Carbon S, Cherry J, Drabkin H, et al. The Gene Ontology knowledgebase in 2023. Genetics. 2023;224(1):iyad031.
20. Ye Q, Taleb S, Zhao J, Zhao Y. Emerging role of BMPs /BMPR2 signaling pathway in treatment for pulmonary fibrosis. Biomed Pharmacother. 2024;178:117178.
21. Wang Z, Zhao H. TMEM176B prevents and alleviates bleomycin-induced pulmonary fibrosis via inhibiting transforming growth factor β-Smad signaling. Heliyon. 2024;10(15):e035444.
22. Sikkeland L, Ueland T, Lund M, Durheim M, Mollnes T. A role for the terminal C5–C9 complement pathway in idiopathic pulmonary fibrosis. Front Med (Lausanne). 2023;10:1236495.
23. Suzuki A, Sakamoto K, Nakahara Y, Enomoto A, Hino J, Ando A, et al. BMP3b is a novel antifibrotic molecule regulated by Meflin in lung fibroblasts. Am J Respir Cell Mol Biol. 2022;67(4):446–58.
24. Yeo HJ, Ha M, Shin DH, Lee HR, Kim YH, Cho WH. Development of a novel biomarker for the progression of idiopathic pulmonary fibrosis. Int J Mol Sci. 2024;25(1):599.
25. Abraham D. Role of endothelin in lung fibrosis. Eur Respir Rev. 2008;17(109):145–50.
26. Ghanem M, Justet A, Jaillet M, Vasarmidi E, Boghanim T, Hachem M, et al. Identification of FGFR4 as a regulator of myofibroblast differentiation in pulmonary fibrosis. Am J Physiol Lung Cell Mol Physiol. 2024;327(6): L818–l30.
27. Bouros E, Filidou E, Arvanitidis K, Mikroulis D, Steiropoulos P, Bamias G, et al. Lung fibrosis-associated soluble mediators and bronchoalveolar lavage from idiopathic pulmonary fibrosis patients promote the expression of fibrogenic factors in subepithelial lung myofibroblasts. Pulm Pharmacol Ther. 2017;46:78–87.
28. Vilar-Gomez E, Sookoian S, Pirola CJ, Liang T, Gawrieh S, Cummings O, et al. ADH1B*2 is associated with reduced severity of nonalcoholic fatty liver disease in adults, independent of alcohol consumption. Gastroenterology. 2020;159(3):929–43.
29. Gao N, Chen J, Qi B, Zhao T, Guo Y, Fang Y, et al. Effects of gene polymorphisms, metabolic activity, and content of alcohol dehydrogenase and acetaldehyde dehydrogenases on prognosis of hepatocellular carcinoma patients. Turk J Gastroenterol. 2022;33(7):606–14.
30. Xu G, Gong Y, Lu F, Wang B, Yang Z, Chen L, et al. Endothelin receptor B enhances liver injury and proinflammatory responses by increasing G-protein-coupled receptor kinase-2 expression in primary biliary cholangitis. Sci Rep. 2022;12(1):19772.
31. Zhang Y, Gai X, Li Y, Chen Z, Zhang X, Qiao W, et al. Autocrine GDF10 inhibits hepatic stellate cell activation

via BMPR2/ALK3 receptor to prevent liver fibrosis. Adv Sci (Weinh). 2025:e2500616.
32. Yu C, Wang F, Jin C, Wu X, Chan WK, McKeehan WL. Increased carbon tetrachloride-induced liver injury and fibrosis in FGFR4-deficient mice. Am J Pathol. 2002;161(6):2003–10.
33. Liao WJ, Lin H, Cheng CF, Ka SM, Chen A, Yang RB. SCUBE1-enhanced bone morphogenetic protein signaling protects against renal ischemia-reperfusion injury. Biochim Biophys Acta Mol Basis Dis. 2019;1865(2):329–38.
34. Kuppe C, Ibrahim MM, Kranz J, Zhang X, Ziegler S, Perales-Patón J, et al. Decoding myofibroblast origins in human kidney fibrosis. Nature. 2021;589(7841):281–6.
35. Zha Y, Li Y, Ge Z, Wang J, Jiao Y, Zhang J, et al. ADAMTS8 promotes cardiac fibrosis partly through activating EGFR-dependent pathway. Front Cardiovasc Med. 2022;9:797137.
36. Meng Q, Bao D, Liu S, Huang J, Guo M, Dai B, et al. ADAM Metallopeptidase domain 19 promotes skin fibrosis in systemic sclerosis via neuregulin-1. Mol Med. 2024;30(1):269.
37. Meng X, Clews J, Kargas V, Wang X, Ford RC. The cystic fibrosis transmembrane conductance regulator (CFTR) and its stability. Cell Mol Life Sci. 2017;74(1):23-38.
38. Shih DQ, Zheng L, Zhang X, Zhang H, Kanazawa Y, Ichikawa R, et al. Inhibition of a novel fibrogenic factor Tl1a reverses established colonic fibrosis. Mucosal Immunol. 2014;7(6):1492-503.
39. Wang JH, Zhao LF, Wang HF, Wen YT, Jiang KK, Mao XM, et al. GenCLiP 3: mining human genes' functions and regulatory networks from PubMed based on co-occurrences and natural language processing. Bioinformatics. 2019.
40. Epstein Shochet G, Brook E, Bardenstein-Wald B, Shitrit D. TGF-beta pathway activation by idiopathic pulmonary fibrosis (IPF) fibroblast derived soluble factors is mediated by IL-6 trans-signaling. Respir Res. 2020;21(1):56.
41. Saraswat M, Joenvaara S, Tohmola T, Sutinen E, Vartiainen V, Koli K, et al. Label-free plasma proteomics identifies haptoglobin-related protein as candidate marker of idiopathic pulmonary fibrosis and dysregulation of complement and oxidative pathways. Sci Rep. 2020;10(1):7787.
42. Paulin F, Doyle TJ, Fletcher EA, Ascherman DP, Rosas IO. Rheumatoid Arthritis-Associated Interstitial Lung Disease and Idiopathic Pulmonary Fibrosis: Shared Mechanistic and Phenotypic Traits Suggest Overlapping Disease Mechanisms. Rev Invest Clin. 2015;67(5):280-6.
43. Triggianese P, Conigliaro P, De Martino E, Monosi B, Chimenti MS. Overview on the Link Between the Complement System and Auto-Immune Articular and Pulmonary Disease. Open Access Rheumatol. 2023;15:65-79.
44. Warheit-Niemi HI, Edwards SJ, SenGupta S, Parent CA, Zhou X, O'Dwyer DN, et al. Fibrotic lung disease inhibits immune responses to staphylococcal pneumonia via impaired neutrophil and macrophage function. JCI Insight. 2022;7(4).
45. Wang L, Zhu M, Li Y, Yan P, Li Z, Chen X, et al. Serum Proteomics Identifies Biomarkers Associated With the Pathogenesis of Idiopathic Pulmonary Fibrosis. Mol Cell Proteomics. 2023;22(4):100524.
46. Palumbo-Zerr K, Zerr P, Distler A, Fliehr J, Mancuso R, Huang J, et al. Orphan nuclear receptor NR4A1 regulates transforming growth factor-beta signaling and fibrosis. Nat Med. 2015;21(2):150-8.
47. Okamoto T, Mathai SK, Hennessy CE, Hancock LA, Walts AD, Stefanski AL, et al. The relationship between complement C3 expression and the MUC5B genotype in pulmonary fibrosis. Am J Physiol Lung Cell Mol Physiol. 2018;315(1):L1-L10.
48. She YX, Yu QY, Tang XX. Role of interleukins in the pathogenesis of pulmonary fibrosis. Cell Death Discov. 2021;7(1):52.
49. Okuda R, Matsushima H, Aoshiba K, Oba T, Kawabe R, Honda K, et al. Soluble intercellular adhesion molecule-1 for stable and acute phases of idiopathic pulmonary fibrosis. Springerplus. 2015;4:657.
50. Kakuta S, Shibata S, Iwakura Y. Genomic structure of the mouse 2',5'-oligoadenylate synthetase gene family. J Interferon Cytokine Res. 2002;22(9):981-93.
51. Reyfman PA, Walter JM, Joshi N, Anekalla KR, McQuattie-Pimentel AC, Chiu S, et al. Single-Cell Transcriptomic Analysis of Human Lung Provides Insights into the Pathobiology of Pulmonary Fibrosis. Am J Respir Crit Care Med. 2019;199(12):1517-36.
52. Habermann AC, Gutierrez AJ, Bui LT, Yahn SL, Winters NI, Calvi CL, et al. Single-cell RNA sequencing reveals profibrotic roles of distinct epithelial and mesenchymal lineages in pulmonary fibrosis. Sci Adv. 2020;6(28):eaba1972.
53. Wynn TA. Integrating mechanisms of pulmonary fibrosis. J Exp Med. 2011;208(7):1339-50.
54. Chen R, Zhu H, Zhang X, Li L, Xu J, Tan Z, et al. Characterization and Functional Analysis of the 17-Beta Hydroxysteroid Dehydrogenase 2 (hsd17b2) Gene during Sex Reversal in the Ricefield Eel (Monopterus albus). Int J Mol Sci. 2024;25(16).
55. Jin P, Cai J, Chen N, Liu Y, Zhao H, Wang Y, et al. TGF-beta/snail-mediated epithelial-to-mesenchymal transition disrupts estradiol metabolism through suppressing the HSD17B2 expression in endometriotic epithelial cells. Biochem Biophys Res Commun. 2025;771:151964.
56. Montgomery C, Pei Z, Watkins PA, Miziorko HM. Identification and characterization of an extramitochondrial human 3-hydroxy-3-methylglutaryl-CoA lyase. J Biol Chem. 2012;287(40):33227-36.
57. Geng X, Dufu K, Hutchaleelaha A, Xu Q, Li Z, Li CM, et al. Increased hemoglobin-oxygen affinity ameliorates bleomycin-induced hypoxemia and pulmonary fibrosis. Physiol Rep. 2016;4(17).
58. Singh S, Bernal Astrain G, Hincapie AM, Goudreault M, Smith MJ. Complex interplay between RAS GTPases and

RASSF effectors regulates subcellular localization of YAP. EMBO Rep. 2024;25(8):3574-600.
59. Grossi E, Marchese FP, Gonzalez J, Goni E, Fernandez-Justel JM, Amadoz A, et al. A lncRNA-mediated metabolic rewiring of cell senescence. Cell Rep. 2025;44(6):115747.
60. Li J, Zhai X, Sun X, Cao S, Yuan Q, Wang J. Metabolic reprogramming of pulmonary fibrosis. Front Pharmacol. 2022;13:1031890.
61. Lin Y, Xu Z. Fibroblast Senescence in Idiopathic Pulmonary Fibrosis. Front Cell Dev Biol. 2020;8:593283.